Low Temperature Physics/Fizika Nizkikh Temperatur, 2017, v. 43, No. 6, pp. 819–827

Polarization dependence of microwave-induced magnetoconductivity oscillations in a two-dimensional electron gas on liquid helium

Yu.P. Monarkha

B. Verkin Institute for Low Temperature Physics and Engineering of the National Academy of Sciences of Ukraine
47 Nauky Ave., Kharkiv 61103, Ukraine
E-mail: monarkha@ilt.kharkov.ua

Received September 21, 2016, published online April 25, 2017

The dependence of radiation-induced dc magnetoconductivity oscillations on the microwave polarization is theoretically studied for a two-dimensional system of strongly interacting electrons formed on the surface of liquid helium. Two different theoretical mechanisms of magnetooscillations (the displacement and inelastic models) are investigated. We found that both models are similarly sensitive to a change of circular polarization, but they respond differently to a change of linear polarization. Theoretical results are compared with the recent observation of a photoconductivity response at cyclotron-resonance harmonics.

PACS: **73.40.–c** Electronic transport in interface structures;
73.20.–r Electron states at surfaces and interfaces;
78.67.–n Optical properties of low-dimensional, mesoscopic, and nanoscale materials and structures;
73.25.+i Surface conductivity and carrier phenomena.

Keywords: 2D electron gas, microwave radiation, magnetoconductivity oscillations, zero resistance states.

1. Introduction

Microwave-induced resistance oscillations (MIRO) and zero resistance states (ZRS) of a 2D electron gas which were discovered in high quality GaAs/AlGaAs heterostructures [1–4] subjected to a perpendicular magnetic field have attracted much interest. For a quite arbitrary microwave (MW) frequency $\omega > \omega_c$ (here ω_c is the cyclotron frequency), these oscillations are governed by the ratio ω/ω_c. In the vicinity of $\omega/\omega_c = m$, where m is an integer, resistivity $[\rho_{xx}(B)]$ and conductivity $[\sigma_{xx}(B)]$ curves have an asymmetrical shape. At strong enough power and low temperatures, the minima of these curves positioned near $\omega/\omega_c = m + 1/4$ evolve into zero-resistance states. A large number of theoretical mechanisms have been proposed to explain these magneto-oscillations [5–10] (for a review, see [11]), but the subject is still under debate. The ZRS can be explained [12] by an assumption that the longitudinal linear response conductivity σ_{xx} is negative in appropriate ranges of the magnetic field **B**, regardless of details of a microscopic mechanism.

Different MW-induced magnetoconductivity oscillations and ZRS are observed in the nondegenerate 2D electron system formed on the free surface of liquid helium [13,14] if the intersubband excitation frequency $(\Delta_2 - \Delta_1)/\hbar \equiv \omega_{2,1}$ coincides with the MW frequency ω (here, Δ_1 and Δ_2 are the energies of the ground and first excited surface subbands, respectively). The explanation of this phenomenon [15,16] is based on nonequilibrium population of the second surface subband caused by the MW resonance which triggers quasielastic intersubband scattering against or along the driving force, depending on the relation between $\hbar\omega_{2,1}$ and the in-plane excitation energy $m\hbar\omega_c$. It was found that these oscillations vanished if ω was substantially different from $\omega_{2,1}$, which means that the origin of these oscillations is different from that of MIRO observed in semiconductor heterostructures. It is interesting that states of surface electrons (SEs) with negative σ_{xx} are unstable which experimentally results in redistribution of SEs [17]. Under these conditions, the system can form a density-domain structure [18] caused by strong Coulomb interaction of SEs.

Two most elaborated mechanisms of MIRO proposed for semiconductor systems (“displacement” [5,6] and “inelastic” [7,8]) are based on photon-assisted scattering. In the displacement model, a displacement of the electron

orbit center $X' - X$ which follows from energy conservation for photon-assisted scattering by impurities depends strongly on the relation between $\hbar\omega$ and $m\hbar\omega_c$. In the inelastic mechanism, photon-assisted scattering to high Landau levels ($n' - n = m$) changes the electron distribution function $f(\varepsilon)$ near $\varepsilon \approx \varepsilon_{n'}$ [here $\varepsilon_n = \hbar\omega_c(n+1/2)$ is the Landau spectrum] which affects usual impurity scattering. A theoretical analysis [19] indicates that both these mechanisms potentially can reveal themselves in the nondegenerate system of SEs on liquid helium. Still, observation of these effects in this system requires significantly higher MW power, because the mass of free electrons M is much larger than the effective mass of semiconductor electrons M^* ($M^*/M \sim 0.06$).

In recent experiments [20], the amplitude of the MW electric field E_{ac} was significantly increased (up to $E_{ac} \approx 10$ V/cm) and ω/ω_c-periodic dc magnetoconductivity oscillations induced by the MW were observed in the nondegenerate 2D electron system on the surface of liquid ^{4}He. This proved the universality of the effect of MIRO. A preliminary theoretical analysis given there have shown that the observation can be explained by an oscillatory correction to the electron distribution function caused by photon-assisted scattering (the inelastic model) affected by strong internal forces.

For semiconductor experiments on MIRO, the important point is the polarization sensitivity or immunity of the microwave magnetoresistance response [21]. Theoretical models discussed in the literature usually predict different microwave polarization sensitivity in the radiation-induced oscillations. Therefore, an appropriate experimental study can be a test for the theory. For SEs on liquid helium, MW-induced magnetoconductivity oscillations were investigated theoretically [19] only for the linear polarization fixed parallel to the dc-electric field. Therefore, additional theoretical investigation on polarization dependence of MW-induced oscillations is required.

In this work, we report the theory of dc magnetoconductivity oscillations of SEs on liquid helium induced by the MW field of an arbitrary polarization (linear and circular). For both displacement and inelastic mechanisms of MIRO, photon-assisted scattering of SEs by ripplons (capillary wave quanta) is considered using Landau–Floquet states which include the MW field in an exact way. This allows us to find the polarization dependence of MIRO in a simple analytical form. Strong Coulomb interaction of SEs is taken into account considering an ensemble of electrons moving fast in the electric field $\mathbf{E}_f$ of the fluctuational origin [22,23]. A comparison of our results with observations [20] indicates that, for a given amplitude of the MW field ($E_{ac} \approx 10$ V/cm), the inelastic model results in sufficiently large magnetoconductivity oscillations similar to those reported experimentally.

2. Landau–Floquet states for an arbitrary MW polarization

SEs on liquid helium are bound in a 1D potential well formed by the liquid repulsion barrier $U_0 \approx 1$ eV, image attraction potential $U(z) = -\Lambda/z$, and the potential of a pressing electric field $eE_\perp z$. The image potential is rather weak because $\Lambda = e^2(\epsilon-1)/4(\epsilon-1)$ and the liquid helium dielectric constant ϵ is very close to unity (for liquid ^{4}He, $\epsilon - 1 \simeq 0.057$). Therefore, in the ground subband electrons are gliding above the surface at a height of about 100 Å. At low temperatures ($T \lesssim 0.5$ K), the population of higher subbands can be neglected. Here we concentrate on the in-plane motion of SEs, assuming that the wave function of vertical motion $h(z)$ is well known, and the intersubband excitation frequency $\omega_{2,1}$ is substantially higher than the MW frequency ω.

We consider the magnetic field $\mathbf{B}$ directed perpendicular to the electron layer and choose the Landau gauge for the vector potential. Then, in the presence of a MW electric field $\mathbf{E}_{mw}(t)$ and a dc electric field $\mathbf{E}_{dc}$ directed along the x axis, the Hamiltonian of an electron can be written as

$$H = \frac{1}{2M}\left\{\hat{p}_x^2 + \left(\hat{p}_y + \frac{eB}{c}x\right)^2\right\} + eE_{dc}x + eE_{mw}^{(x)}(t)x + eE_{mw}^{(y)}(t)y. \quad (1)$$

For this Hamiltonian, the wave equation can be solved in an exact way using a generalization of the well-known nonperturbative method (for a recent example, see Ref. 24). The wave equation can be satisfied by

$$\psi = \varphi(x - X - \xi, t)\, e^{\frac{i}{\hbar}p_y(y-\zeta)} \times \exp\left\{\frac{i}{\hbar}M\left[\dot{\xi}(x - X - \xi) + \dot{\zeta}(y - \zeta)\right] + \frac{i}{\hbar}\eta(t)\right\}, \quad (2)$$

where

$$X = -\frac{cp_y}{eB} - \frac{eE_{dc}}{M\omega_c^2},$$

and the surface area is set to unity. The functions $\xi(t)$, $\zeta(t)$ and $\eta(t)$ are found from conditions chosen to reduce the wave equation to the conventional oscillator equation. After lengthy algebra we arrive at

$$M\ddot{\xi} + M\omega_c^2\xi + M\omega_c\dot{\zeta} + eE_{mw}^{(x)}(t) = 0, \quad (3)$$

$$M\ddot{\zeta} + eE_{mw}^{(y)}(t) = 0. \quad (4)$$

The function $\eta(t)$ can be written as $\eta(t) = \eta_0(t) + \eta_X(t)$, where

$$\dot{\eta}_0 = \frac{M}{2}\dot{\xi}^2 + \frac{M}{2}\dot{\zeta}^2 - \frac{M}{2}\omega_c^2\xi^2 - eE_{mw}^{(x)}\xi - eE_{mw}^{(y)}\zeta - M\omega_c\xi\dot{\zeta},$$

and

$$\eta_X = -M\omega_c X\left[\zeta(t)-\zeta(0)\right] - X\int_0^t eE_{mw}^{(x)}(t')\,dt'. \quad (5)$$

The $\xi(t)$ represents the classical motion of an electron in a magnetic field forced by an ac electric field, while $\zeta(t)$ represents a 1D electron motion in the field $E_{mw}^{(y)}(t)$.

Thus, instead of $\varphi(x,t)$ entering Eq. (2), we can use usual eigenfunctions $\varphi_n(x)$ of an oscillator Hamiltonian

$$\varphi_n(x,t) = \varphi_n(x)\exp\left(-i\frac{\varepsilon_{n,X}}{\hbar}t\right),$$

$$\varepsilon_{n,X} = \varepsilon_n + eE_{dc}X + \frac{e^2E_{dc}^2}{2M\omega_c^2}. \quad (6)$$

Therefore, the Landau–Floquet eigenfunctions of the Hamiltonian given in Eq. (1) can be represented as

$$\psi_{n,X} = \varphi_n(x-X-\xi,t)\,e^{-iXy/l_B^2}e^{F_X(t)}e^{i\theta(x,y,t)}, \quad (7)$$

where

$$F_X(t) = -\frac{i}{\hbar}MX\dot{\xi} - \frac{i}{\hbar}X\int_0^t eE_{ac}^{(x)}(t')\,dt' + \frac{i}{\hbar}M\omega_c X\zeta(0), \quad (8)$$

and the exact form of the function $\theta(x,y,t)$ independent of n and X is not important for the following consideration.

Specifying $\mathbf{E}_{mw}(t)$, we shall consider

$$E_{mw}^{(x)} = aE_{ac}\cos\omega t, \quad E_{mw}^{(y)} = bE_{ac}\sin\omega t, \quad (9)$$

where E_{ac} is the amplitude of the MW field, and, generally, a and b are arbitrary parameters. For particular cases, we assume that a can be 0 or 1, and b can be 0 or ±1. In this way, we can describe two linear polarizations [parallel ($a=1,\ b=0$) and perpendicular ($a=0,\ b=1$) to the dc electric field] and two circular polarizations ($a=1$, $b=\pm1$). Respectively, we define the polarization index $s = \|, \perp, +, -$, where the first two symbols ($\|$ and $\perp$) correspond to linear polarizations, and the last two symbols (+ and –) correspond to circular polarizations. Now we have

$$\zeta = \frac{beE_{ac}}{M\omega^2}\sin\omega t, \quad \xi = \frac{(a\omega+b\omega_c)}{(\omega^2-\omega_c^2)}\frac{eE_{ac}}{M\omega}\cos\omega t, \quad (10)$$

$$F_X(t) = i\lambda\frac{X}{l_B}\frac{\omega_c(a\omega_c+b\omega)}{(\omega^2-\omega_c^2)}\sin\omega t, \quad (11)$$

where $l_B^2 = \hbar c/eB$, and $\lambda = eE_{ac}l_B/\hbar\omega$. Using these definitions, one can determine the matrix elements for electron scattering probabilities.

3. Scattering probabilities

At low temperatures, SEs on liquid helium interact with capillary-wave excitations (ripplons). The electron-ripplon interaction Hamiltonian (ripplons represent a sort of 2D phonons) is usually described as

$$V_I = \sum_{\mathbf{q}} U_q Q_q\left(b_{-\mathbf{q}} + b_{\mathbf{q}}^{\dagger}\right)e^{-i\mathbf{q}\cdot\mathbf{r}}, \quad (12)$$

where $b_{\mathbf{q}}^{\dagger}$ and $b_{\mathbf{q}}$ are creation and destruction operators of ripplons, U_q is the electron-ripplon coupling [23], $Q_q^2 = \hbar q/2\rho\omega_{r,q}$, $\omega_{r,q} \simeq \sqrt{\alpha/\rho}q^{3/2}$ is the ripplon spectrum, α and ρ are the surface tension and mass density of liquid helium, respectively.

Scattering probabilities depend on matrix elements $(e^{-i\mathbf{q}\cdot\mathbf{r}})_{n',X',n,X}$ which now acquire additional time-dependent factors: one factor comes directly from $\exp\left[F_X(t)\right]$ of Eq. (7), and another factor $\exp(-iq_x\xi)$ appears because of the change of the integration variable $x = x_1 + X + \xi$. Gathering these two factors, one can find

$$(e^{-i\mathbf{q}\cdot\mathbf{r}})_{n',X',n,X} = e^{-i\beta_{s,\mathbf{q}}\sin(\omega t+\gamma)} \times$$

$$\times\,\delta_{X,X'-l_B^2q_y}(e^{-iq_xx})_{n',X';n,X}^{(0)}, \quad (13)$$

where

$$\beta_{s,\mathbf{q}} = \frac{\lambda\omega_c l_B}{(\omega^2-\omega_c^2)}\sqrt{q_y^2(a\omega_c+b\omega)^2 + q_x^2(a\omega+b\omega_c)^2}, \quad (14)$$

$$\tan\gamma = \frac{q_x(a\omega+b\omega_c)}{q_y(a\omega_c+b\omega)},$$

and $(e^{-iq_xx})_{n',X';n,X}^{(0)}$ are matrix elements in the absence of the MW field. Here the first term under the sign of the square root of Eq. (14) originates from the factor $\exp[F_X(t)]$, and the second is from $\exp(-iq_x\xi)$. Then, using the Jacobi–Anger expansion $e^{iz\sin\varphi} = \sum_k J_k(z)\,e^{ik\varphi}$ [here $J_k(z)$ is the Bessel function], the procedure of finding scattering probabilities can be reduced to a quite usual treatment.

The probability of electron scattering $n, X \to n', X'$ with the momentum exchange $\mathbf{q}$ due to ripplon creation (+) and destruction (–) can be found as

$$w_{\mathbf{q},n,X\to n',X'}^{(\pm)} = \frac{2\pi}{\hbar}\left|C_{\mathbf{q}}^{(\pm)}\right|^2 I_{n,n'}^2(x_q)\,\delta_{X,X'-l_B^2q_y} \times$$

$$\times\sum_{k=-\infty}^{\infty} J_k^2(\beta_{s,\mathbf{q}})\,\delta(\varepsilon_{n',X'} - \varepsilon_{n,X} - k\hbar\omega \pm \hbar\omega_{r,q}), \quad (15)$$

where $C_{\mathbf{q}}^{(\pm)} = U_qQ_q\left[n_{\pm\mathbf{q}}^{(r)} + 1/2 \pm 1/2\right]^{1/2}$, $n_{\pm\mathbf{q}}^{(r)}$ is the number of ripplons with the wave vector $\pm\mathbf{q}$, $\varepsilon_{n,X}$ is from Eq. (6),

$$I^2_{n,n'}(x_q)=\frac{\min(n,n')!}{\max(n,n')!}x_q^{|n'-n|}\times$$
$$\times\exp(-x_q)\left[L^{|n'-n|}_{\min(n,n')}(x_q)\right]^2, \qquad (16)$$

$L^m_n(x_q)$ are the associated Laguerre polynomials, and $x_q=q^2l_B^2/2$ is a dimensionless variable. We note that for Landau–Floquet states, matrix elements of Eq. (13) fix the displacement of the orbit center to the same value $X'-X=q_yl_B^2$ as that of usual scattering. It is instructive also that, considering the MW field in a classical way, we still found that the energy exchange in Eq. (15) occurs by MW quanta $k\hbar\omega$.

Energies of ripplons $\hbar\omega_{r,q}$ involved in one-ripplon scattering processes are usually much smaller than typical electron energies, and we can use a quasi-elastic treatment of electron-ripplon scattering. Therefore, in the energy conservation delta-function, we shall set $\hbar\omega_{r,q}$ to zero. This allows us to write the whole probability as a sum $w_{\mathbf{q}}=w^{(+)}_{\mathbf{q}}+w^{(-)}_{\mathbf{q}}$ neglecting a small difference between $C^{(+)}_{\mathbf{q}}$ and $C^{(-)}_{\mathbf{q}}$.

Introducing Landau level densities of states, the average probability of electron scattering $\overline{w}_{\mathbf{q}}$ with the momentum exchange $\mathbf{q}$, can be found in terms of the dynamic structure factor (DSF) $S(q,\Omega)$ of a nondegenerate 2D electron gas

$$\overline{w}_{\mathbf{q}}=\frac{2C_q^2}{\hbar^2}\sum_{k=-\infty}^{\infty}J_k^2(\beta_{s,\mathbf{q}})S(q,k\omega-q_yV_H), \qquad (17)$$

where $C_q\simeq U_qQ_qN_{r,q}^{1/2}$, $N_{r,q}$ is the ripplon distribution function, $V_H=cE_{dc}/B$ is the absolute value of the Hall velocity which enters the frequency argument due to $eE_{dc}(X'-X)=\hbar q_yV_H$,

$$S(q,\Omega)=\frac{2}{\pi\hbar Z_{\|}}\sum_{n,n'}I^2_{n,n'}(x_q)\int d\varepsilon e^{-\varepsilon/T_e}g_n(\varepsilon)g_{n'}(\varepsilon+\hbar\Omega), \qquad (18)$$

T_e is the electron temperature, $Z_{\|}$ is the partition function for the Landau spectrum ε_n, and $-g_n(\varepsilon)$ is the imaginary part of the single-electron Green's function. For the Gaussian shape of level densities [25],

$$g_n(\varepsilon)=\frac{\sqrt{2\pi}\hbar}{\Gamma_n}\exp\left[-\frac{2(\varepsilon-\varepsilon_n)^2}{\Gamma_n^2}\right],$$

where Γ_n is the Landau level broadening. For SEs on liquid helium, at low temperatures Γ_n is usually much smaller than T and $\hbar\omega_c$.

4. The displacement model

Using Eq. (17), the dc magnetoconductivity σ_{xx} of SEs under MW radiation can be found directly considering the current density

$$j_x=-en_e\sum_{\mathbf{q}}(X'-X)_{\mathbf{q}}\,\overline{w}_{\mathbf{q}}=-en_el_B^2\sum_{\mathbf{q}}q_y\overline{w}_{\mathbf{q}}.$$

Therefore, the effective collision frequency

$$\nu_{\rm eff}=-\frac{1}{MV_H}\sum_{\mathbf{q}}\hbar q_y\overline{w}_{\mathbf{q}}(V_H) \qquad (19)$$

defines $\sigma_{xx}\simeq e^2n_e\nu_{\rm eff}/M\omega_c^2$. Expanding Eq. (19) in V_H yields the linear dc magnetoconductivity in terms of the derivative of the DSF $S'=\partial S/\partial\Omega$. The property $S(q,-\Omega)=\exp(-\hbar\Omega/T_e)S(q,\Omega)$ allows us to represent the effective collision frequency as a sum $\nu_{\rm eff}=\sum_{k=0}^{\infty}\nu_k$, where

$$\nu_0=\frac{1}{MT_e}\sum_{\mathbf{q}}q_y^2C_q^2J_0^2(\beta_{s,\mathbf{q}})S(q,0), \qquad (20)$$

and

$$\nu_k=\frac{2\left(1-e^{-k\hbar\omega/T_e}\right)}{M\hbar}\sum_{\mathbf{q}}q_y^2C_{\mathbf{q}}^2J_k^2(\beta_{s,\mathbf{q}})S'(q,k\omega) \qquad (21)$$

for $k>0$. Here we neglected a small term $(\hbar/T_e)e^{-k\hbar\omega/T_e}S(q,k\omega)$ as compared to $S'(q,k\omega)$. In Eq. (20), the derivative $S'(q,0)$ was transformed employing the relationship $S'(q,0)=(\hbar/2T_e)S(q,0)$. It is instructive that in the nonperturbative method, the MW field affects also the usual contribution to the effective collision frequency ν_0 due to the factor $J_0^2(\beta_{s,\mathbf{q}})$.

SEs on liquid helium represent a highly correlated electron system because the average Coulomb interaction energy per an electron $e^2\sqrt{\pi n_e}$ (here n_e is the electron density) is usually much larger than the average kinetic energy T. In this case, each electron is affected by a strong internal electric field $\mathbf{E}_f$ of fluctuational origin [26]. The typical value of the fluctuational field depends strongly on the electron temperature and density: $E_f^{(0)}\simeq 3\sqrt{T_e}n_e^{3/4}$. Self-energy effects (collision broadening of Landau levels) can be combined with the Coulomb effect by considering the DSF of an ensemble of electrons moving fast in the fluctuational field [22,23]. Therefore, to model the effect of Coulomb interaction on MW-induced conductivity oscillations we shall use the DSF obtained previously [23] for strongly interactions electrons

$$S(q,\Omega)\simeq\frac{2\sqrt{\pi}}{Z_{\|}}\sum_{n,n'}e^{-\varepsilon_n/T_e}\frac{I^2_{n,n'}}{\gamma_{n,n'}}\times$$
$$\times\exp\left[-\frac{\left[\Omega-(n'-n)\omega_c-\phi_n\right]^2}{\gamma^2_{n,n'}}\right], \qquad (22)$$

where

$$\hbar\gamma_{n,n'}=\sqrt{\Gamma^2_{n,n'}+x_q\Gamma_C^2},\quad \phi_n=\frac{\Gamma_n^2+x_q\Gamma_C^2}{4T_e\hbar}, \qquad (23)$$

$2\Gamma_{n,n'}^2 = \Gamma_n^2 + \Gamma_{n'}^2$, and $\Gamma_C = \sqrt{2}eE_f^{(0)}l_B$. In most cases, the parameter ϕ_n can be neglected. Thus, the strong Coulomb interaction of SEs results in a broadening of DSF maxima which occur at $\Omega \to (n'-n)\omega_c$. In the presence of MW radiation of a circular polarization, the employment of Eq. (22) gives absolutely correct description of the many-electron effect on magnetooscillations. For a linear MW polarization, this procedure is a reasonable approximation.

With the exception of the cyclotron resonance (CR) condition ($\omega_c \to \omega$), the parameter $\beta_{s,\mathbf{q}}$ defined in Eq. (14) is small and one can expand the Bessel functions in $\beta_{s,\mathbf{q}}$. In this case, the main term of Eq. (20) transforms into the well known result of the self-consistent Born approximation [27]. In spite of small values of $\beta_{s,\mathbf{q}}$, the contribution from ν_1 can be substantial because it contains the derivative of the function $S(q,\omega)$ having sharp maxima. Using dimensionless coupling function $U_c(x_q) = U_q l_B^2/\Lambda$ (its exact form is given in Refs. 16, 19) and Eq. (22), we arrive at

$$\nu_{1,s} = \lambda^2 \frac{\sqrt{\pi}T\nu_R}{\hbar\omega_c}\left(1-e^{-\hbar\omega/T_e}\right)\chi_s F(B), \qquad (24)$$

$$F(B) = -\sum_{n,n'} \frac{e^{-\varepsilon_n/T_e}}{Z_{\|}} \int_0^\infty dx_q U_c^2(x_q) x_q I_{n,n'}^2 \times$$

$$\times \frac{\omega/\omega_c - m - \phi_n/\omega_c}{(\gamma_{n,n'}/\omega_c)^3} \exp\left[-\frac{(\omega - m\omega_c - \phi_n)^2}{\gamma_{n,n'}^2}\right], \qquad (25)$$

where $\nu_R = \Lambda^2/8\pi\hbar\alpha l_B^4$ is a characteristic collision frequency, $m = n'-n$, and χ_s is a dimensionless polarization factor with the polarization index $s = \|, \perp, +, -$. For two linear polarizations,

$$\chi_{\|} = \frac{\omega_c^2(3\omega_c^2+\omega^2)}{(\omega^2-\omega_c^2)^2}, \quad \chi_{\perp} = \frac{\omega_c^2(3\omega^2+\omega_c^2)}{(\omega^2-\omega_c^2)^2}, \qquad (26)$$

and for two circular polarizations,

$$\chi_{\pm} = \frac{4\omega_c^2(\omega \pm \omega_c)^2}{(\omega^2-\omega_c^2)^2}. \qquad (27)$$

Besides the small factor λ^2, the quantum form of Eq. (24) contains two large factors $T/\hbar\omega_c$ and $(\omega_c/\gamma_{n,n'})^2$. It should be noted that in the ultra-quantum limit $\hbar\omega \gg T_e$, Eq. (24) with the linear MW polarization $s = \|$ transforms into the result found previously [19] using the conventional perturbation theory, if we set

$$\left\langle \mathbf{E}^2 \right\rangle = 4\pi \frac{N_{mw}(\omega)}{V}\hbar\omega \to E_{ac}^2/2,$$

where $N_{mw}(\omega)$ is the number of photons with the frequency ω in the volume V. This confirms the validity of the approach to description of probabilities of photon-assisted scattering using Landau–Floquet states.

The MW-induced correction to the effective collision frequency of noninteracting electrons can be obtained from Eqs. (24) and (25) by setting the Coulomb broadening Γ_C to zero. In this case, $\gamma_{n,n'}$ is independent of x_q, and, therefore, the derivative of the Gaussian [which can be formed in the lowest line of Eq. (25)] can be moved out from the integrand. Thus, the shape of MW-induced oscillations near $\omega/\omega_c = m$ represents a simple derivative of a Gaussian. Formally, in the limit of strong broadening of the Gaussians the positions of minima approach the condition $\omega/\omega_c(B) \to m + 1/4$, which agrees with observations. The Coulomb interaction broadens the derivative of Gaussians and involves it into averaging over x_q because $\gamma_{n,n'}$ of Eq. (23) becomes dependent on x_q.

The Eq. (24) indicates that, for two different polarizations described by indexes s and s', the ratio $\nu_{1,s}/\nu_{1,s'} = \chi_s/\chi_{s'}$. When changing the parameter ω/ω_c the ratio $\chi_\perp/\chi_\|$ varies from 1.86 ($\omega/\omega_c = 2$) to 3 ($\omega/\omega_c \to \infty$). For circular polarizations, the ratio χ_+/χ_- decreases with m: from 9 ($\omega/\omega_c = 2$) to 1 ($\omega/\omega_c \to \infty$). Results of numerical evaluations of $\nu_{1,s}$ obtained for two linear polarizations are shown in Fig. 1. Here the main parameters of the SE system are the same as those in the experiment [20]. The many-electron treatment of the displacement model results in the broadening of MW-induced oscillations which agrees with experimental data. Still, the amplitude of oscillations caused by the MW field directed parallel to E_{dc} is approximately an order of magnitude smaller than the amplitude observed. As expected, the MW field with the perpendicular polarization ($s = \perp$) results in dc magnetoconductivity oscillations having a substantially larger amplitude.

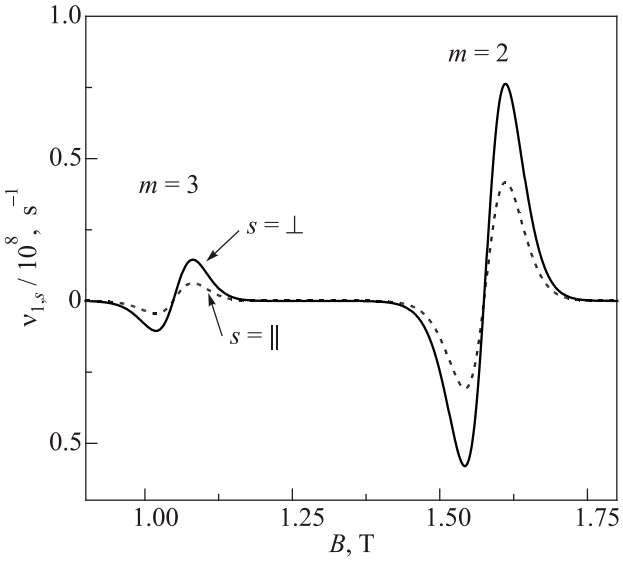

Fig. 1. An oscillatory contribution to the effective collisions frequency calculated for two different MW polarizations: $s = \|$ (dashed) and $s = \perp$ (solid). The conditions are the following: $E_{ac} = 10$ V/cm, $n_e = 17 \cdot 10^6$ cm^{-2}, $\omega/2\pi = 88.34$ GHz, and $T = 0.56$ K (liquid ^{4}He).

For the CR condition ($\omega_c \simeq \omega$), $\chi_\perp / \chi_\parallel \simeq 1$ and the photoconductivity is immune to a change of linear polarization. In this case, the parameter $\beta_{\|,\mathbf{q}}$ entering the Bessel function of Eq. (24) can be simplified as

$$\beta_{\|,\mathbf{q}} \simeq \lambda \frac{\omega_c^2}{(\omega^2 - \omega_c^2)} q l_B. \tag{28}$$

As noted previously [28] [in the brief report, there is a small misprint in the expression similar to Eq. (28)], the parameter $\beta_{\|,\mathbf{q}}$ increases much when $\omega_c \to \omega$ and, generally, it is impossible to expand the Bessel functions. Moreover, according to the expression for the DSF $S(q, k\omega)$, sharp Gaussian maxima appear for the all k at $k\omega = (n' - n)\omega_c$, and, if $\omega_c \to \omega$, it is necessary to take account of the all terms in the sum $\sum_{k=0}^{\infty} \nu_k$. A formal inclusion of a damping parameter in the classical equations for ξ and ζ can reduce the number of ν_k to be taken into account.

Results of numerical calculations are shown in Fig. 2. As a damping parameter, here we chosen the classical collision frequency of SEs. This figure illustrates that at a fixed value of $\omega - \omega_c \neq 0$, the sum over k converges quite rapidly. Still, each next term in the sum $\sum_{k=0}^{\infty} \nu_k$ has its own extrema which are closer to the point $\omega_c = \omega$. Therefore, in the vicinity of the resonance, a substantial number of ν_m should be taken into account.

As mentioned above, these calculations does not depend on the orientation of the linear polarization of the microwave field. On the contrary, for the circular polarization with $s = -$, the strong enhancement of the parameter $\beta_{s,\mathbf{q}}$ caused by the CR vanishes and one can restrict calculations to ν_1 given by Eqs. (24) and (25). For the chosen amplitude of the MW field, corresponding oscillatory features could not be seen on the scale of Fig. 2.

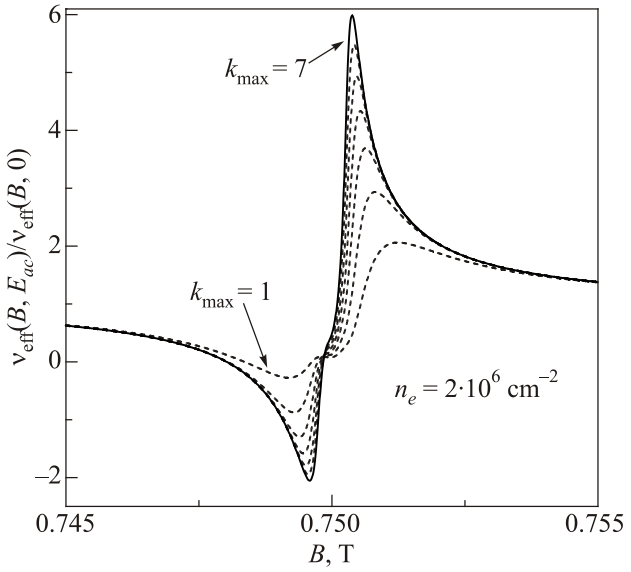

Fig. 2. Contributions from partial sums $\sum_{k=0}^{k_{\max}} \nu_k$ to $\nu_{\rm eff}$ normalized vs the magnetic field for a sequence of $k_{\max}$: from $k_{\max} = 1$ to $k_{\max} = 7$ (solid). The conditions are the following: $T = 0.2$ K (liquid ^{4}He), $n_e = 2\cdot 10^6$ cm^{-2}, and $E_{ac} = 0.05$ V/cm.

Results shown in Fig. 2 are obtained assuming $T_e = T$. Still, under the CR condition, the system of SEs on liquid helium is strongly heated [29] and the electron temperature as a function of $\omega - \omega_c$ usually has a sharp maximum [30]. Because $\nu_0 \propto 1/T_e$, the wavy variations of $\sigma_{xx}(B)$ induced by photon-assisted scattering are expected to appear at the bottom of a broad minimum caused by electron heating.

5. The inelastic model

In the displacement model discussed above, it is assumed that the electron distribution function $f(\varepsilon)$, entering the average probability of the momentum exchange $\overline{w}_{\mathbf{q}}$ and the effective collision frequency $\nu_{\rm eff}$ of Eq. (19), coincides with the equilibrium distribution function $Z_\|^{-1} e^{-\varepsilon/T_e}$. Still, photon-assisted scattering from a level n to a higher level n' selected by the condition $\varepsilon_{n'} - \varepsilon_n \simeq \hbar\omega$ might increase the population of the level n'. Moreover, if the energy exchange with the medium (in our case, the ripplon energy) can be neglected in the energy conservation delta-function, the sharp structure of the level density $g_n(\varepsilon)$ could make a sharp shape of $f(\varepsilon)$ at $\varepsilon \simeq \varepsilon_{n'}$ which eventually results in MW-induced magnetoconductivity oscillations. This is the inelastic model, introduced in Ref. 7.

The photon energy $\hbar\omega$ and the magnetic field B usually select two Landau levels with $\varepsilon_{n'} - \varepsilon_n \simeq \hbar\omega$. In the ultraquantum limit important for SEs on liquid helium, this allows us to consider a simple two-level model for obtaining a correction to the distribution function. When analyzing the average transition rate up ($n \to n'$) and the all transition rates down ($n' \to n$), we can represent them as integral forms ($\int d\varepsilon \int d\varepsilon' ...$) similar to that of Eqs. (17) and (18) using the Landau level density of states. Then, disregarding the Coulomb interaction, for an energy $\varepsilon' \simeq \varepsilon_{n'}$, it is possible to obtain the rate-balance condition

$$f_{n'}(\varepsilon') = \frac{f_n(\varepsilon' - \hbar\omega) r_{n,n'}(\varepsilon')}{\nu_{n'}^{(2R)} + r_{n,n'}(\varepsilon')}, \tag{29}$$

where

$$r_{n,n'}(\varepsilon') = \frac{\lambda^2 T}{2\hbar} \overline{\chi}_s \nu_R P_{n,n'} g_n(\varepsilon' - \hbar\omega)$$

is the excitation rate,

$$P_{n,n'} = \int_0^\infty U_c^2(x_q) I_{n,n'}^2(x_q) dx_q,$$

$$\overline{\chi}_\perp = \overline{\chi}_\| = \frac{2\omega_c^2(\omega_c^2 + \omega^2)}{(\omega^2 - \omega_c^2)^2}, \quad \overline{\chi}_\pm = \chi_\pm, \tag{30}$$

$\nu_{n'}^{(2R)}$ is the inelastic transition rate from n' to the all $n < n'$ caused by two-ripplon emission processes [31]. In the distribution function $f_{n'}(\varepsilon')$, the subscript n' indicates

that its argument ε' is close to $\varepsilon_{n'}$. Dimensionless integrals $P_{n,n'}$ describe the strength of the electron-ripplon coupling in the presence of a strong magnetic field.

Here the polarization immunity $\overline{\chi}_\perp = \overline{\chi}_\parallel$ appears because the transition rate $r_{n,n'}$ is finite in the limit $E_{dc} \to 0$ and integration over the angle of the vector $\mathbf{q}$ results in equal averaging of q_x^2 and q_y^2 entering $\beta_{s,\mathbf{q}}$ of Eq. (14) (note that the probability of scattering is proportional to $\beta_{s,\mathbf{q}}^2$). In the displacement model, one have to expand $\overline{w}_\mathbf{q}$ in $q_y V_H$ up to a linear term which results in unequal averaging of q_x^2 and q_y^2. This leads to the linear MW polarization sensitivity of the displacement model in radiation-induced oscillations.

Direct electron transitions between different Landau levels accompanied by one-ripplon creation or destruction are practically impossible because the typical value of $|\mathbf{q}|$ which follows from energy conservation is much larger than l_B^{-1} (the dimensionless parameter $x_q \gg 1$). Still, there are transitions from a level n' to lower levels accompanied by emission of pairs of short wavelength ripplons with $|\mathbf{q}+\mathbf{q}'| \lesssim l_B^{-1} \ll q, q'$. According to Ref. 31, $\nu_{n'}^{(2R)}$ can be written as

$$\nu_{n'}^{(2R)} = \frac{2}{l_B^2 \hbar} \sum_{n=0}^{n'-1} \sum_{\mathbf{q}} W_q^2 Q_q^4 (N_{r,q}+1)^2 \, \delta(\varepsilon_{n'} - \varepsilon_n - 2\hbar\omega_q), \tag{31}$$

where W_q is the coupling function for two-ripplon scattering. In terms of continuous variables ε' and ε, the $\nu_{n'}^{(2R)}$ varies slow within the width of a Landau level since $\Gamma_n \ll \hbar\omega_c$. This allows us to use the form of Eq. (31) in Eq. (29).

The Eq. (29) reminds the solution of the rate equation of a two-level model usually obtained in quantum optics. The second term in the denominator of this equation is caused by backward electron transitions accompanied by emission of a photon. Firstly, we note that in the absence of the inelastic decay rate $\nu_{n'}^{(2R)}$, the solution satisfies the saturation condition $f_{n'}(\varepsilon') = f_n(\varepsilon' - \hbar\omega)$ which is quite obvious. Secondly, a sharp shape of $f_{n'}(\varepsilon')$ appears when the inelastic scattering rate is stronger then the excitation rate: $\nu_{n'}^{(2R)} \gg r_{n,n'}$. In this case, the single-electron treatment yields $f_{n'}(\varepsilon') \propto g_n(\varepsilon' - \hbar\omega)$ because $f_n(\varepsilon)$ can be approximately set to the equilibrium function. This is the reason why the mechanism discussed here is called the inelastic model.

In the inelastic model, the correction to σ_{xx} is usually obtained from the conductivity equation which contains the derivative $\partial f / \partial \varepsilon$. This picture is instructive to see how the derivative of maxima appears in the final result. Still, according to Eq. (19), the initial form of the effective collision frequency contains the derivative $g'_{n'}(\varepsilon) = \partial g_{n'} / \partial \varepsilon$. Therefore, in the ultra-quantum limit ($n \to 0$), the correction to the effective collision frequency induced by additional population of higher Landau levels can be written as

$$\nu_{mw} = \frac{4\nu_R T \hbar\omega_c}{\pi\hbar^2} \sum_{n'=1}^{\infty} P_{n',n'} \int d\varepsilon f_{n'}(\varepsilon) g_{n'}(\varepsilon) g'_{n'}(\varepsilon). \tag{32}$$

Here we neglected the overlapping of different Landau levels. The Eq. (32) is obtained in the same way as Eqs. (20), (21). The form of ν_{mw} with the derivative $\partial f / \partial \varepsilon$ can be found from Eq. (32) using integration by parts [19].

Assuming low exitation regime ($r_{n,n'} \ll \nu_{n'}^{(2R)}$) and inserting $f_{n'}(\varepsilon)$ in Eq. (32), we find

$$\nu_{mw} = \pi\lambda^2 \overline{\chi}_s \nu_R^2 T^2 \hbar\omega_c \sum_{n'=1}^{\infty} \frac{P_{n',n'} P_{0,n'}}{\nu_{n'}^{(2R)} \Gamma_{n'} G_{0,n'}} \times \times \frac{2(n'\hbar\omega_c - \hbar\omega)}{G_{0,n'}^2} \exp\left[-\frac{(n'\hbar\omega_c - \hbar\omega)^2}{G_{0,n'}^2} \right], \tag{33}$$

where $G_{n,n'}^2 = \Gamma_{n,n'}^2 - \Gamma_{n'}^2 / 4$. The Eq. (33) indicates that, in the inelastic model, the shape of MW-induced magnetoconductivity oscillations represents the derivative of a Gaussian similar to that of the displacement model [Eq. (24)]. In contrast with the displacement model, additional large parameters $\nu_R / \nu_{n'}^{(2R)}$ and $T / G_{0,n}$ appear in the expression for ν_{mw} which makes MIRO more pronounced.

For experimental conditions [20], the Eq. (33) results in conductivity variations near $\omega / \omega_c = n' = m$ which are substantially sharper than those observed. Respectively, the amplitude of oscillations is much higher than in the experiment. This discrepancy can be attributed to the effect of strong Coulomb interaction which broadens the Gaussians and accordingly reduces the amplitude of oscillations. Unfortunately, a strict description of this effect is very difficult because now the fluctuational electric field affects the both $f_{n'}(\varepsilon)$ and $g'_{n'}(\varepsilon)$. In order to describe the many-electron effect qualitatively, we can introduce a correction to the energy exchange caused by a fluctuational electric field $eE_f(X' - X) \simeq \hbar\mathbf{q} \cdot \mathbf{u}_f$ (here $\mathbf{u}_f$ is a drift velocity) and average the both quantities $f_{n'}$ and $g'_{n'}$ over $\mathbf{E}_f$, independently. This yields an additional broadening of the parameter

$$G_{0,n'}^2 \to \Gamma_{0,n'}^2 + x_{q'} \Gamma_C^2 - \frac{\Gamma_{n'}^4}{4(\Gamma_{n'}^2 + x_q \Gamma_C^2)} \tag{34}$$

which becomes dependent on x_q (the integration variable of $P_{n',n'}$) and $x_{q'}$ (the integration variable of $P_{0,n'}$). The later means that the derivative of Gaussians now enters the integrand of the double-integral $\int dx_q \int dx_{q'} \ldots$, and calculations become more complicated. Moreover, the averaging over the fluctuational field changes the factor

$$\frac{1}{\Gamma_{n'}} \to \frac{\Gamma_{n'}^2}{(\Gamma_{n'}^2 + x_q \Gamma_C^2)^{3/2}} \tag{35}$$

reducing electron scattering. As a result, conductivity variations near $\omega / \omega_c = m$ aquire the broadening which agrees

with experimental data. Still, the new factor of Eq. (35) leads to a more rapid decrease of the amplitude of oscillations with m than it is observed. Thus, Eq. (34) gives a reasonable approximation describing the effect of Coulomb broadening of conductivity oscillations induced by the MW, while the replacement of Eq. (35) is expected to be improved in a more accurate treatment. For example, the procedure of averaging of ν_{mw}, taken in the form containing the derivative $\partial f / \partial \varepsilon$, results in a different replacement: $\Gamma_{n'} \to (\Gamma_{n'}^2 + x_q \Gamma_C^2)^{1/2}$.

In the inelastic model discussed here, the amplitude of oscillations does not depend on the orientation of the linear polarization of the microwave field because $\overline{\chi}_\perp = \overline{\chi}_\parallel$. This is in contrast with the results found for the displacement model and illustrated in Fig. 1. For semiconductor systems, the same conclusion was drown previously [8]. Regarding the circular polarization, the both mechanisms of MIRO give the same dependence on the polarization index $s = \pm$ described by the factors $\overline{\chi}_\pm = \chi_\pm$. This dependence on the polarization index follows directly from the classical parameter $\xi(t)$ entering the Landau–Floquet wave function. According to Eq. (10), the amplitude of $\xi(t)$ depends strongly on the sign of b. The most obvious example is that the classical CR vanishes if $b = -1$ ($s = -$). The difference between χ_+ and χ_- is strong for a few lowest $m = 2, 3, ...$, and it decreases with ω / ω_c.

Typical magnetoconductivity oscillations, obtained for the inelastic model including the Coulomb interaction as described in Eqs. (34) and (35), are shown in Fig. 3. Here we considered two circular polarizations. The amplitude of oscillations is significantly larger if the polarization vector rotates in phase with respect to the cyclotron rotation (in our notations $s = +$). A similar dependence of MW induced oscillations on a choice of the circular polarization were reported for different versions of the displacement model applied to a degenerate 2D electron system [32,33]. Dependencies of the amplitude of magnetoconductivity oscillations on the MW polarization obtained here are valid only for small values of the parameter $\beta_{s,\mathbf{q}}$ given in Eq. (14), when we can neglect multi-photon processes and expand the Bessel function $J_1(\beta_{s,\mathbf{q}})$. For the system of SEs on liquid helium, these conditions are fulfilled if $m > 1$.

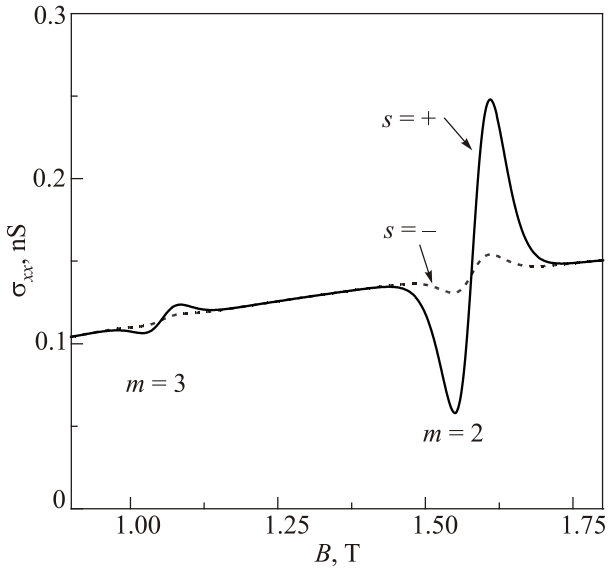

Fig. 3. Magnetoconductivity of SEs on liquid helium exposed to the MW field with $E_{ac} = 10$ V/cm calculated for two circular polarizations: $s = -$ (dashed) and $s = +$ (solid). Other conditions are the same as in Fig. 1

It should be noted that in a semiconductor 2D electron system, the microwave induced resistance oscillations and the zero resistance regions are notably immune to the sense of circular polarization [34]. This can be regarded as a crucial test for theories. Obviously, the circular polarization immunity of the photoconductivity can not be reconciled with the displacement and inelastic mechanisms of MIRO. On the other hand, for SEs on liquid helium, the many-electron treatment of the inelastic model results in an oscillation-amplitude consistent with experimental observations [20]. One may assume that magnetoconductivity oscillations observed for SEs on liquid helium and MIRO reported for GaAs/AlGaAs heterostructures are caused by different mechanisms. Therefore, circular-polarization-dependent measurements of photoconductivity response of SEs at CR harmonics are of great interest.

6. Conclusions

Summarizing, we developed a theoretical approach which enabled us to obtain the dependence of MW-induced dc magnetoconductivity oscillations on the MW polarization in a nondegenerate 2D electron system bound to the free surface of liquid helium. Probabilities of photon-assisted scattering of surface electrons by capillary-wave quanta (ripplons) are shown to be well described using Landau–Floquet states which include the microwave field and the dc electric field in a nonperturbative exact way. The photoconductivity is found expanding the average probability of a momentum exchange in the dc electric field. Photon-assisted scattering affects the magnetoconductivity in two different ways by changing directly the momentum exchange between SEs and ripplons (the displacement model), and changing the distribution function of excited Landau levels (the inelastic model). The effect of strong Coulomb interaction is described considering an ensemble of electrons moving fast in a quasi-uniform internal electric field of the fluctuational origin.

We found that the ratio of oscillation-amplitudes obtained for MW fields of different polarizations is described by a simple analytical form. Contributions of the both theoretical models to the photoconductivity of SEs are shown to be very sensitive to a change of circular polarization, if the parameter ω / ω_c is not large. For different circular polarizations, the ratio of oscillation-amplitudes is the same in the both models. This is caused by the nature of photon-assisted scattering whose strength depends on the ampli-

tude of classical motion sensitive to a circular polarization. On the contrary, the displacement and inelastic models respond differently to a change of the direction of the MW field having a linear polarization. In the displacement model, the oscillation-amplitude depends strongly on whether the MW electric field is parallel or perpendicular to the dc electric field. At the same time, the inelastic model is insensitive to a change of linear polarization. Therefore, an experiment with MW fields of different circular polarizations could be a test for photon-assisted scattering, while an experiment with different linear polarizations could be a test for particular mechanisms of magnetooscillations. Numerical calculations performed for experimental conditions [20] indicate that MW-induced dc magnetoconductivity oscillations observed can be explained by an oscillatory correction to the electron distribution function caused by photon-assisted scattering affected by strong Coulomb forces.

1. M.A. Zudov, R.R. Du, J.A. Simmons, and J.R. Reno, *Phys. Rev. B* **64**, 201311(R) (2001).
2. R. Mani, J.H. Smet, K. von Klitzing, V. Narayanamurti, W.B. Johnson, and V. Umansky, *Nature* **420**, 646 (2002).
3. M.A. Zudov, R.R. Du, L.N. Pfeiffer, and K.W. West, *Phys. Rev. Lett.* **90**, 046807 (2003).
4. C.L. Yang, M.A. Zudov, T.A. Knuuttila, R.R. Du, L.N. Pfeiffer, and K.W. West, *Phys. Rev. Lett.* **91**, 096803 (2003).
5. A.C. Durst, S. Sachdev, N. Read, and S.M. Girvin, *Phys. Rev. Lett.* **91**, 086803 (2003).
6. V. Ryzhii and R. Suris, *J. Phys.*: *Condens. Matter* **15**, 6855 (2003).
7. I.A. Dmitriev, A.D. Mirlin, and D.G. Polyakov, *Phys. Rev. Lett.* **91**, 226802 (2003).
8. I.A. Dmitriev, M.G. Vavilov, I.L. Aleiner, A.D. Mirlin, and D.G. Polyakov, *Phys. Rev. B* **71**, 115316 (2005).
9. A.A. Koulakov and M.E. Raikh, *Phys. Rev. B* **68**, 115324 (2003).
10. S.A. Mikhailov, *Phys. Rev. B* **83**, 155303 (2011).
11. I.A. Dmitriev, A.D. Mirlin, D.G. Polyakov, and M.A. Zudov, *Rev. Mod. Phys.* **84**, 1709 (2012).
12. A.V. Andreev, I.L. Aleiner, and A.J. Millis, *Phys. Rev. Lett.* **91**, 056803 (2003).
13. D. Konstantinov and K. Kono, *Phys. Rev. Lett.* **103**, 266808 (2009).
14. D. Konstantinov and K. Kono, *Phys. Rev. Lett.* **105**, 226801 (2010).
15. Yu.P. Monarkha, *Fiz. Nizk. Temp.* **37**, 108 (2011) [*Low Temp. Phys.* **37**, 90 (2011)]; Yu.P. Monarkha, *Fiz. Nizk. Temp.* **37**, 829 (2011) [*Low Temp. Phys.* **37**, 655 (2011)].
16. Yu.P. Monarkha, *Fiz. Nizk. Temp.* **38**, 579 (2012) [*Low Temp. Phys.* **38**, 451 (2012)].
17. D. Konstantinov, A. Chepelianskii, and K. Kono, *J. Phys. Soc. Jpn.* **81**, 093601 (2012).
18. Yu.P. Monarkha, *Fiz. Nizk. Temp.* **42**, 657 (2016) [*Low Temp. Phys.* **42**, 441 (2016)].
19. Yu.P. Monarkha, *Fiz. Nizk. Temp.* **40**, 623 (2014) [*Low Temp. Phys.* **40**, 482 (2014)].
20. R. Yamashiro, L.V. Abdurakhimov, A.O. Badrutdinov, Yu.P. Monarkha, and D. Konstantinov, *Phys. Rev. Lett.* **115**, 256802 (2015).
21. R.G. Mani, A.N. Ramanayaka, and W. Wegscheider, *Phys. Rev. B* **84**, 085308 (2011).
22. Yu.P. Monarkha, E. Teske, and P. Wyder, *Phys. Rep.* **370**, issue 1, 1 (2002).
23. Yu.P. Monarkha and K. Kono, *Two-Dimensional Coulomb Liquids and Solids*, Springer-Verlag, Berlin (2004).
24. K. Park, *Phys. Rev. B* **69**, 201301(R) (2004).
25. R.R. Gerhardts, *Surf. Sci.* **58**, 227 (1976).
26. M.I. Dykman and L.S. Khazan, *Zh. Eksp. Teor. Fiz.* **77**, 1488 (1979) [*Sov. Phys. JETP* **50**, 747 (1979)].
27. T. Ando and Y. Uemura, *J. Phys. Soc. Jpn.* **36**, 959 (1974).
28. Yu.P. Monarkha, *Phys. Rev. B* **91**, 121402(R) (2015).
29. A.O. Badrutdinov, L.V. Abdurakhimov, and D. Konstantinov, *Phys. Rev. B* **90**, 075305 (2014).
30. Yu.P. Monarkha, *Fiz. Nizk. Temp.* **41**, 652 (2015) [*Low Temp. Phys.* **41**, 508 (2015)].
31. Yu.P. Monarkha, S.S. Sokolov, A.V. Smorodin, and N. Studart, *Fiz. Nizk. Temp.* **36**, 711 (2010) [*Low Temp. Phys.* **36**, 565 (2010)].
32. M. Torres and A. Kunold, *Phys. Rev. B* **71**, 115313 (2005).
33. I.I. Lyapilin and A.E. Patrakov, Phys. Met. Metallogr., **102**, 560 (2006).
34. J.H. Smet, B. Gorshunov, C. Jiang, L. Pfeiffer, K. West, V. Umansky, M. Dressel, R. Meisels, F. Kuchar, and K. von Klitzing, *Phys. Rev. Lett.* **95**, 116804 (2005).